Journal of Materials Chemistry A

ROYAL SOCIETY OF CHEMISTRY

HIGHLIGHT

View Article Online
View Journal | View Issue

Cite this: J. Mater. Chem. A, 2023, 11, 12425

Microporous metal–organic frameworks for the purification of propylene

Feng Xie,[a] Hao Wang *[b] and Jing Li *[ab]

Separation of propylene from its analogous hydrocarbons such as propane is of great importance in the petrochemical industry to produce valuable chemical feedstocks with desired purity. However, the well-established method currently used for industrial propane/propylene separation is energy intensive. It involves repeated cycling in the cryogenic and high-pressure distillation process and requires multiple columns and high reflux ratios because of the very similar physical properties of the two species. Thus, it is identified as one of the most capital- and energy-intensive processes. Adsorptive separation based on porous adsorbents is regarded as an alternative energy-efficient technology to replace or supplement the traditional heat-driven cryogenic distillation processes. In this context, metal–organic frameworks (MOFs) have emerged as the most promising candidates for propane/propylene separation, taking into consideration their unique tunability with respect to pore geometry and pore functionality. In this highlight, we summarize the latest advancement in developing MOFs as physisorbents for the separation and purification of propylene from propane, with a focus on those that demonstrate selective molecular exclusion and propane-selective adsorption. We discuss the adsorption preferences related to the material design and separation mechanisms, and review the existing challenges. Finally, we offer our perspectives on various strategies for the future design of MOFs that hold true potential for propylene purification under industrial settings.

Received 30th November 2022
Accepted 3rd January 2023

DOI: 10.1039/d2ta09326j

rsc.li/materials-a

10th Anniversary Statement

On the occasion of the 10th anniversary of *Journal of Materials Chemistry A*, we would like to offer our heartfelt congratulations for its remarkable achievement and success since its first issue published in January 2013. With joy and excitement, we have witnessed the rapid growth of the Journal over the past 10 years, and its support to, and impact on, the field of materials research and development. It has also been a privilege and pride for us to serve the journal with multiple roles: as reviewers, authors, and members of the advisory board. We are delighted and proud for the opportunities to contribute to the Journal, and we have enjoyed interacting with many others associated with the journal. It is our hope and belief that *Journal of Materials Chemistry A* will continue to excel and lead in the next 10 years and beyond.

1. Introduction

Propylene is a primary olefin feedstock in the petrochemical industry for the manufacture of a variety of chemical commodities, including polypropylene.[1,2] Due to its good resistance to fatigue, heat, and organic solvents, polypropylene has been widely used for films, fibers, containers, and packaging.[3] Propylene is typically produced from refineries: either as the by-product of steam cracking of naphtha or as an off-gas from fluid catalytic cracking units, with a propylene purity of 50–60% for the former and 80–87% for the latter.[4–6] Propylene in the streams is accompanied by various impurities, in particular propane. Before it is used to produce polypropylene or acrylonitrile, the monomer needs to be purified to reach a desired purity (*e.g.*, polymer grade, >99.5%), which typically involves the separation of propylene from the propylene/propane mixtures.[7] However, propylene and propane have very similar physical properties such as molecular size, volatility, and boiling point. The industrially established method for propylene/propane separation involves repeated distillation–compression cycling in giant C3 splitter towers of up to 300 feet high with over 200 trays, which is reported as the most capital- and energy-intensive process in the chemical industry.[2] The energy consumption of this separation process is estimated at 12.9 GJ per ton of propylene.[8,9] In the high demand to improve the energy efficiency of the separation process, adsorptive separation based on porous materials has attracted great interest as an alternative technology with lower energy input. It is estimated that advanced non-thermal separation techniques could result in ~15–38% energy savings compared to the conventional cryogenic distillation process,[10,11] as such technologies effectively separate paraffin and

[a]Department of Chemistry and Chemical Biology, Rutgers University, Piscataway, New Jersey, 08854, USA. E-mail: jingli@rutgers.edu

[b]Hoffmann Institute of Advanced Materials, Shenzhen Polytechnic, 7098 Liuxian Boulevard, Shenzhen, Guangdong 518055, P.R. China. E-mail: wanghao@szpt.edu.cn

olefin molecules based on their chemical affinity or size rather than the difference in boiling point and thus can be carried out under mild conditions, significantly reducing the operating costs and energy inputs.[12] The key players of these new technologies are the porous solid or permeable membranes, which are made of porous materials with nanosized voids. The effectiveness and efficiency of these technologies rely on the separation performance of the porous media, which are determined by their internal pore structures.[13,14]

Conventional porous materials such as zeolites, silica gel, activated carbon and alumina have long been used as adsorbents,[15,16] and play important roles in many industrial applications involving cooling, drying, filtration, separation, and purification, to name a few. However, the lack of precise control of their pore structure limits their separation performance for challenging gas separations, particularly for gas molecules with very similar chemical and physical properties.[17] As such, developing advanced adsorbent materials with a pore structure of high modulating accuracy is much needed, especially given the operational simplicity and tremendous energy savings of the adsorptive separation technology.[18,19] In this context, microporous metal–organic frameworks (MOFs) have demonstrated strong potential to meet the challenges of these very important separations[20,21] due to their well-known excellent modularity, high porosity, and systematically tunable functionality.[13,22–24] The modular nature makes them an ideal platform to tailor the pore environment. The porosity and surface chemistry of MOFs can be easily tuned by rational selection and combination of building blocks with targeted geometries and functions.[21,25] Using organic linkers and metal nodes with different sizes allows precise control of the pore aperture of MOFs at the molecular or atomic level.[26] Various MOFs have been investigated for the separation of propane/propylene over the past few decades (Fig. 1). A number of them have clearly outperformed traditional adsorbents.[7,12,27]

Concerning adsorption and separation of propane and propylene, most of the MOFs reported to date are propylene-selective.[7,36,37] Propylene is preferentially adsorbed from the mixture due to several reasons, for example, as a result of strong host–guest interaction with MOFs having unsaturated metal ions or because of its smaller molecular dimensions making it easier to be accommodated by MOFs with small pore apertures. However, because the desired product is propylene, the propylene-selective MOFs will inevitably undergo a desorption process that suffers from high energy consumption and operation complexity. An adsorbent that preferentially adsorbs propane is much more desirable for such a process, as it will not only generate high-purity propylene in one step but also greatly reduces the energy and adsorbent amount.

In this highlight, we will give an overview of the most recent work on adsorptive separation of propylene from propane using MOF adsorbents, with an emphasis on the structure design strategy and four types of separation mechanisms. In addition, we will select representative MOFs in each category and discuss their adsorption preference (*e.g.*, propane-selective or propylene-selective) and significance for propylene purification. Finally, we will review the current concerns and provide an outlook on the future developments of material design strategies and structure–property relationships in MOFs that are important to realize energy-efficient propylene purification based on adsorptive separation technology.

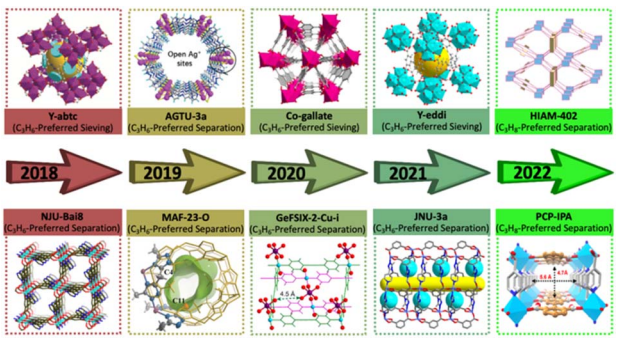

Fig. 1 Timeline of the latest development of representative MOFs for propylene/propane separation. Y-abtc: reproduced with permission.[6] Copyright 2018, Wiley-VCH. NJU-Bai8: reproduced with permission.[28] Copyright 2018, Elsevier. AGTU-3a: reproduced with permission.[29] Copyright 2019, Royal Society of Chemistry. MAF-23-O: reproduced with permission.[30] Copyright 2019, Wiley-VCH. Co-gallate: reproduced with permission.[7] Copyright 2020, American Chemical Society. GeFSIX-2-Cu-i: reproduced with permission.[31] Copyright 2020, American Chemical Society. Y-eddi: reproduced with permission.[32] Copyright 2021, American Chemical Society. JNU-3a: reproduced with permission.[33] Copyright 2021, Springer Nature. HIAM-402: reproduced with permission.[34] Copyright 2022, American Chemical Society. PCP-IPA: reproduced with permission.[35] Copyright 2022, Springer Nature.

2. Adsorptive separation mechanisms

The adsorption mechanisms for MOF-based separation have been well studied in the past two decades. In general, they can

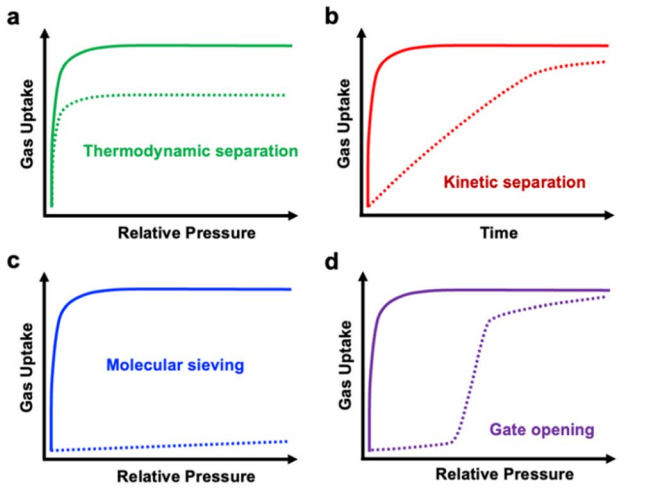

Fig. 2 Illustration of adsorptive separation mechanisms in physisorbents. (a) Thermodynamic driving separation for guests with different affinity sites; (b) kinetic driving separation for guests with different diffusion rates; (c) molecular sieving driving separation for guests with different sizes; (d) gate-opening separation for guests with different interaction strengths.

Table 1 Representative MOFs for propylene purification from propane

Preference	MOF	BET surface area ($m^2\ g^{-1}$)	Pore size (Å)	Uptake amount[a] ($cm^3\ g^{-1}$)		Adsorption heat (Q_{st}, kJ mol^{-1})		Selectivity[b]	Separation mechanism	Ref.
				C_3H_6	C_3H_8	C_3H_6	C_3H_8			
C_3H_6-selective	HIAM-301 ($Y_6(OH)_8(eddi)_3$)	579	4.6	71	7	29.3	27	>100	Molecular sieving	32
	$Zn_3(OH)_2(pzdc)(atz)$	—	4.8	47	2	—	—	>100	Molecular sieving	43
	$Y_6(OH)_8(dbai)_3$	405	4.4	58	2	55	—	>100	Molecular sieving	44
	$Ni[Fe(CN)_5NO]$	543	6.3	80	48	57	32.3	10.5	Thermodynamic	41
	MUF-17 ($Co_5(OH)_2(aip)_4$)	310	5.7	55	45	57.2	22	3.8	Thermodynamic	45
	MFM-520	313	6.6	52	46	48.5	42.3	17	Kinetic	42
	Zn-ATA ($Zn_2(ATA)_3(ATA)$)	349	3.7	32	5	—	—	—	Kinetic	46
	$Ni(aip)(bpy)_{0.5}$	355	6.0	44	10	48.7	—	31	Thermodynamic-kinetic	47
	JNU-3a (Co(mptbdc))	588	5.6	62	50	39	34.9	>100	Gate-opening	33
C_3H_8-selective	PCP-IPA (Co(IPA)(DPG))	487	4.7	50(0.1 bar)	50(0.1 bar)	43.4	50.9	2.5	Thermodynamic	35
	CPM-734c ($Co_2V(OH)(ndc)_3tpbtc$)	1944	9.3	94(0.1 bar)	126(0.1 bar)	30.8	31.5	1.5	Thermodynamic	48
	CPM-736t ($Co_2V(OH)(adc)_3tpt$)	2087	10.9	87(0.2 bar)	141(0.2 bar)	24.7	25.2	1.3	Thermodynamic	48
	$Ni(ADC)(TED)_{0.5}$	679	4.8	40(0.1 bar)	50(0.1 bar)	—	—	6	Thermodynamic	49
	NUM-7 (Mn(tcpe))	—	4.7	50(0.1 bar)	42(0.1 bar)	38.2	40	1.8	Thermodynamic	50
	HIAM-402 ($Zr_6O_4(OH)_4(tcppda)_2$)	1442	8/12	41(0.1 bar)	60(0.1 bar)	31.2	34.5	1.43	Thermodynamic	34

[a] Gas uptake was measured at 298 K and 1.0 bar (or specific pressure). [b] Selectivity was calculated using the IAST model. Acronyms: eddi = 5,5′-(ethene-1,2-diyl)diisophthalic acid; pzdc = 3,5-pyrazoledicarboxylic acid; atz = 3-amino-1,2,4-trizole; dbai = 5-(3,5-dicarboxybenzoylamino) isophthalic acid; aip = 5-aminoisophthalic acid; ATA = 5-aminotetrazole; bpy = 4,4′-bipyridine; mptbdc = 5-(3-methyl-5-(pyridin-4-yl)-4*H*-1,2,4-triazol-4-yl)-1,3-benzenedicarboxylic acid; IPA = isophthalic acid; DPG = *meso*-α,β-di(4-pyridyl) glycol; ndc = 2,6-napthalenedicarboxylic acid; tpbtc = *N*,*N*′,*N*″-tri(4-pyridinyl)-1,3,5-benzenetricarboxamide; adc = azobenzene-4,4′-dicarboxylic acid; tpt = 2,4,6-tri(4-pyridinyl)-1,3,5-triazine; ADC = 9,10-anthracenedicarboxylic acid, TED = triethylenediamine; tcpe = 1,1,2,2-tetra(4-carboxylphenyl)ethylene; tcppda = *N*,*N*,*N*′,*N*′-tetrakis(4-carboxyphenyl)-1,4-phenylene-diamine.

be categorized into four types, namely adsorptions *via* thermodynamic, kinetic, molecular sieving, and gate-opening processes (Fig. 2).[14] Thermodynamic separation is the most common process and has been observed in a large majority of adsorbents. This separation is driven by the differences in adsorption affinity (Fig. 2a), which can be enhanced by pore surface modification with strong and specific binding sites. Other processes, such as kinetic separation (Fig. 2b) and molecular sieving (Fig. 2c), rely on diffusivity difference largely governed by the pore size, which can be optimized by tuning the pore aperture. Molecular sieving is essentially an extreme case of kinetic separation and is the most efficient process to produce high-purity gases with extremely high adsorption selectivity and relatively low energy consumption. In some cases, the separation is achieved by a synergistic effect of thermodynamic and kinetic processes, which requires collaborative control in the interior of adsorbents. In addition, some gas adsorption processes are accompanied by the changes in the crystal structure because of framework flexibility, which are often associated with a gate opening phenomenon that gives rise to selective separation (Fig. 2d).

3. Propylene-selective separation for propylene purification

As stated above, most MOFs reported for propane/propylene separation are propylene-selective, as a result of the smaller molecular size and the unsaturated carbon double bonds of propylene. In this section, we discuss the current progress in propylene-selective separation of propane/propylene by MOFs *via* the four mechanisms mentioned above. The separation performance parameters of representative MOFs, including gas uptake, separation selectivity, and isosteric heat of adsorption, are summarized in Table 1 along with the porosity data of the adsorbents. To enhance the separation efficiency, several strategies have been utilized, such as creating functional sites within MOFs for thermodynamic or kinetic separations, fine-tuning the pore geometry for molecular-sieving based separation, and optimizing the structural flexibility for gate-opening separation.

It has been demonstrated that coordinatively unsaturated metal ions are active binding sites. Generally, electron-rich transition metals interact strongly with unsaturated carbon–carbon bonds. A prototype MOF containing unsaturated metal centers (or OMSs), Cu-BTC (HKUST-1,$Cu_3(BTC)_2$), has been studied thoroughly for its separation of propane/propylene following a thermodynamic mechanism by molecular simulation and experimental methods.[38] Preferential adsorption of propylene over propane was confirmed by higher adsorption capacity and isosteric heat for propylene.[39,40] Very recently, Xie *et al.* developed an ultra-microporous cyanide-based compound, $Ni[Fe(CN)_5NO]$, which features a cavity-like compact pore space with abundant OMSs for highly efficient separation of propylene from propane (Fig. 3a).[41] The material exhibits high propylene/propane selectivity of 10.5 with a remarkable propylene uptake capacity of 80 $cm^3\ g^{-1}$ at 1 bar (Fig. 3b). Its capability for separation was further verified by experimental column breakthrough measurements. Propane was successfully separated from propylene, accompanied by a high propylene capture productivity of 2.30 mol kg^{-1} and a separation factor of 9.6 (Fig. 3c). More importantly, dispersion-corrected density functional theory (DFT) calculations revealed that the selective adsorption of propylene is due to strong host–guest interactions at the OMSs as well as multiple weak hydrogen bonding interactions within the compact pore space.

Making use of the significantly different diffusion rates, Li *et al.* carried out a kinetic separation study of an equimolar mixture of propylene/propane using a highly robust

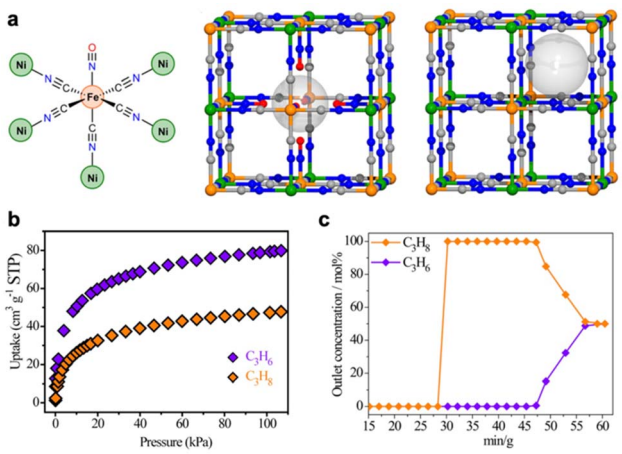

Fig. 3 Representative MOF ($Ni[Fe(CN)_5NO]$) showing thermodynamic separation for propylene-selective purification. (a) The local coordination environment of the nitroprusside linker and different cavities in the crystal structure of $Ni[Fe(CN)_5NO]$. (b) Single-component sorption isotherms of propylene and propane at 298 K. (c) Experimental column breakthrough curves for equimolar propane/propylene mixture in a column packed with $Ni[Fe(CN)_5NO]$ at 298 K and 1 bar. Reproduced with permission.[41] Copyright 2022, Wiley-VCH.

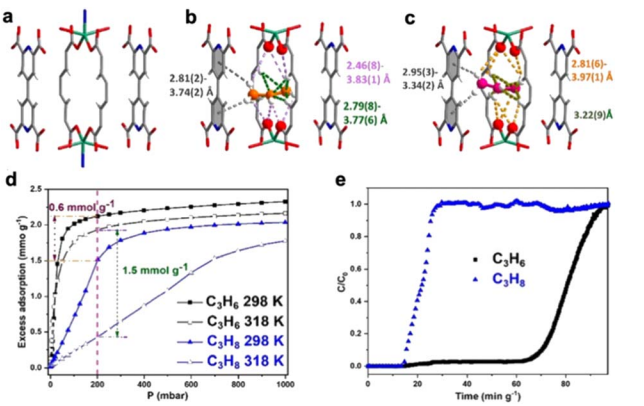

Fig. 4 Representative MOF (MFM-520) showing kinetic separation for propylene-selective purification. (a) Views of the crystal structures of bare MFM-520 and the propylene (b) and propane (c) adsorbed MFM-520. (d) Single-component adsorption isotherms of propylene and propane in MFM-520 at various temperatures. (e) Experimental breakthrough plots for an equimolar propylene/propane mixture at 318 K. Reproduced with permission.[42] Copyright 2021, Wiley-VCH.

microporous material, MFM-520.[42] MFM-520 has a bowtie-shaped small cavity with a dimension of 6.6 × 4.0 × 3.6 Å^3 (Fig. 4a). *In situ* synchrotron single crystal X-ray diffraction and inelastic neutron scattering experiments revealed a series of synergistic host–guest interactions involving hydrogen bonding and π···π stacking interactions, underpinning the cooperative binding of propylene with the pore over propane (Fig. 4b and c). Single-component adsorption experiments of propane and propylene were conducted at different temperatures and the results indicate the presence of sluggish kinetics in propane adsorption, while propylene quickly reached saturation at relatively low pressure (Fig. 4d). Interestingly, while the adsorption capacity of propane in MFM-520 decreases rapidly with increasing temperature, the variation of temperature has a much smaller effect on the uptake of propylene, particularly in the low-pressure region where only small changes were observed for propylene adsorption. For example, the uptakes of propylene at 200 mbar were 2.12 and 1.93 mmol g^{-1} at 298 and 318 K, respectively, whereas for propane the values were 1.51 and 0.43 mmol g^{-1} under the same conditions. The different adsorption kinetics in propane and propylene were well reflected in breakthrough experiments, which demonstrated an efficient kinetic separation of the propane/propylene mixture in MFM-520 (Fig. 4e). The highly confined pore of MFM-520 differentiates the adsorption kinetics between propane and propylene.

By fine-tuning the pore sizes and surface functionality, the efficient molecular-sieving based separation of propylene over propane was also realized by several MOFs. For example, Yu *et al.* recently reported an ultra-microporous MOF, Y-eddi (HIAM-301), that achieved size-sieving of propylene over propane *via* a tailored pore distortion approach.[32] Y-eddi features a distorted cubic cavity (10 × 10 × 10 Å^3) interconnected by small windows (Fig. 5a). Single-component gas adsorption isotherms revealed that Y-eddi could take up a large amount of propylene (3.2 mmol g^{-1} at 298 K and 1 bar) but negligible propane (<0.3 mmol g^{-1}) (Fig. 5b). Such a large adsorption difference resulted in a high IAST selectivity of over 150 for propylene/propane. The simultaneously high propylene uptake and propylene/propane adsorption selectivity make Y-eddi an excellent adsorbent for the separation of propane and propylene. *In situ* neutron powder diffraction (NPD) analysis of C_3D_6-loaded samples showed that C_3D_6 molecules are located mainly in two binding sites through multiple host–guest interactions, thus affording excellent propane/propylene separation performance. Breakthrough experiments on a HIAM-301 packed column further confirmed that polymer-grade propylene can be obtained from an equimolar propane/propylene mixture with a productivity of 38.5 cm^3 g^{-1} (Fig. 5c).

Compared with rigid MOFs that undergo the molecular-sieving mechanism, the adsorbents that exhibit dynamic molecular sieving often show advantage for gas separation due to their faster adsorption–desorption kinetics and thus less energy consumption. For example, Zeng *et al.* recently realized a flexible MOF (JNU-3a) for the dynamic molecular sieving of propylene and propane.[33] Structurally, JNU-3a possesses a 1D channel with an array of pockets lining up to both sides (Fig. 6a). The gourd-shaped aperture between the pocket and the channel is only 3.7 Å, which seems too small for both propylene (4.0 Å) and propane (4.4 Å) to enter the pocket (Fig. 6b and c). Interestingly, the stepwise adsorption was observed in both propylene and propane adsorption isotherms, indicating a guest-induced gate-opening behavior (Fig. 6d). Such unique

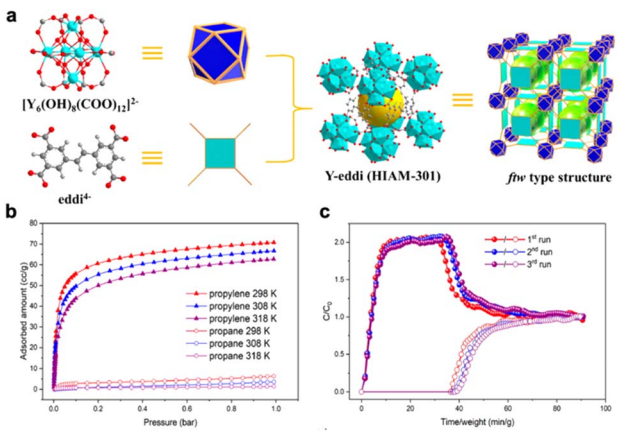

Fig. 5 Representative MOF (Y-eddi) showing selective molecular sieving for propylene-selective purification. (a) Inorganic and organic building units, crystal structure, and topology of Y-eddi. (b) Adsorption isotherms of propylene and propane on Y-eddi at various temperatures. (c) Three consecutive runs of column breakthrough for equimolar propane/propylene binary mixture in a column packed with Y-eddi at room temperature. Propane (filled); propylene (open). Reproduced with permission.[32] Copyright 2021, American Chemical Society.

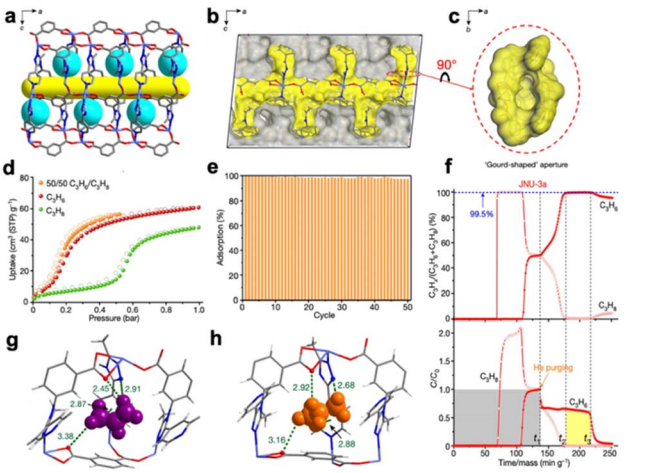

Fig. 6 Representative MOF (JNU-3a) showing gate-opening separation for propylene-selective purification. (a) Pore structure viewed along the *b* axis showing molecular pockets and the 1D channel. (b) Cross-sectional view of the Connolly surface of the void. (c) Close-up view of the 'gourd-shaped' aperture connecting the pocket to the channel. (d) Pure propane, pure propylene, and an equimolar mixture of propylene/propane sorption isotherms of JNU-3a at 303 K. (e) Propylene sorption on JNU-3a over 50 consecutive cycles at 303 K. (f) Breakthrough curves of an equimolar mixture of propylene/propane on JNU-3a. (g) Close-up view of propylene in the single crystal of C_3H_6@JNU-3a. (h) Close-up view of propane in the single crystal of C_3H_8@JNU-3a. Reproduced with permission.[33] Copyright 2021, Springer Nature.

behavior was confirmed by single crystal X-ray diffraction analysis and DFT calculations of propylene- and propane-loaded samples, revealing multiple stronger interactions of the pocket with propylene than with propane (Fig. 6g and h). Most importantly, breakthrough experiments demonstrated that about 53.5 L kg^{-1} of high-purity propylene can be obtained from an equimolar binary mixture of propane/propylene during a single adsorption–desorption cycle (Fig. 6e and f), setting another new record for propane/propylene separation by MOFs.

4. Propane-selective separation for propylene purification

The fact that most of the MOFs reported for propane/propylene separation are propylene-selective can be attributed to several factors: stronger interaction between propylene molecules and metal centers/clusters (*e.g.*, OMS), pore aperture matching (*e.g.*, molecular sieving), or through supramolecular interactions such as π···π stacking (for MOFs without OMS). However, since propylene is the favored component in propane/propylene separation, an additional desorption step is needed if propylene-selective adsorbents are used. Comparably, propane-selective adsorbents would be much more desirable, particularly in cases where minor propane impurities need to be removed from propylene, as they can produce high-purity propylene directly during the adsorption step. This would make the separation process much simpler and more efficient.

Compared to the substantial development of ethane-selective adsorbents, the scarcer progress in propane-selective adsorbents may be attributed to the smaller difference in molecular size and physical properties between propane and propylene.[7,37,51] To target MOFs with the preferential binding of propane over propylene, it is necessary either to create accommodated pore geometry based on the shape-matching to achieve favored recognition of propane or to introduce specific sites for the stronger interactions with propane. Topology evolution by varying linkers and secondary building unit geometries could largely enrich the chemistry of MOFs and generate structures that may possibly show preferential accommodation of propane over propylene. Very recently, Li *et al.* demonstrated the exceptional propane-selective separation of Zr-tcppda (HIAM-402) by the topology regulating approach (Fig. 7a), which is built on an 8-connected hexanuclear Zr_6 cluster and tetrakis(4-carboxyphenyl)-1,4-phenylenediamine and features an sqc topology.[34] HIAM-402 possesses a highly robust framework as well as high porosity and exhibits selective adsorption of propane over propylene. Single-component adsorption isotherms revealed that propane is notably favored at low pressure compared to propylene although the saturation uptakes at 1 bar are similar for the two gases (Fig. 7b). The separation capability by HIAM-402 was demonstrated by column breakthrough measurements using a binary mixture of propane/propylene (5/95; v/v) as a feed (Fig. 7c). The heat of adsorption calculations indicated that the Q_{st} for propane is 34.5 kJ mol^{-1}, higher than that for propylene (31.2 kJ mol^{-1}). The *ab initio* DFT calculations suggested the stronger

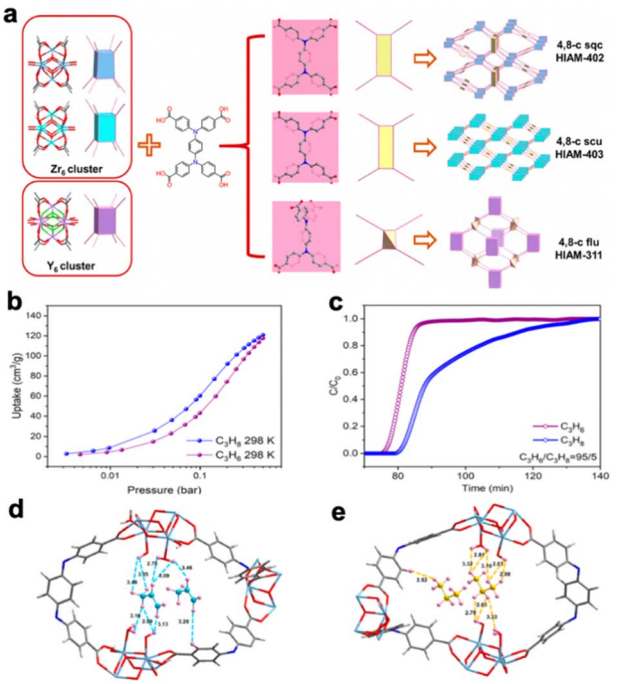

Fig. 7 Representative MOF (HIAM-402) for propane-selective purification. (a) Structure and topology of HIAM-402, HIAM-403, and HIAM-311. (b) Single-component adsorption–desorption isotherms of propane/propylene adsorption isotherms at 298 K. (c) Dynamic breakthrough curves of HIAM-402 for propane/propylene at 298 K and 1 bar. Optimized configuration of adsorbed propylene (d) and propane (e) in the channel of HIAM-402 by *ab initio* calculations. Reproduced with permission.[34] Copyright 2022, American Chemical Society.

supramolecular interactions of propane with the framework based on the shorter H@C_3H_8 bonding with terminal OH and H_2O, through C–H···H interactions and CH···O hydrogen bonds (Fig. 7d and e). Column breakthrough measurements further demonstrated that the compound is capable of one-step purification of C_3H_6 from a $C_3H_6/C_3H_4/C_3H_8$ (94/2/4, v/v/v) ternary mixture.

Very recently, Zhang *et al.* reported an ultra-microporous material (PCP-IPA) consisting of parallel-aligned linearly extending isophthalate units along the 1-D channel. The compound shows efficient propane-selective separation for propylene purification.[35] The material has a suitable pore window of 4.7 × 5.6 $Å^2$ for the accommodation of propane (Fig. 8a). The unique pore size and environment facilitate the directional adsorption of propane through rigid bonds between their aligned hydrogen atoms and the closely parallel-aligned isophthalate units. Although the saturated uptakes of propane and propylene at 1 bar are similar, propane is notably favored at lower pressure compared to propylene (Fig. 8b). Column breakthrough experiments of a propane/propylene mixture indicate that the material is capable of separating propane and propylene (Fig. 8c). Ultra-high purity propylene (99.99%) with a record productivity of 15.23 L kg^{-1} can be obtained directly from the equimolar mixture of propane/propylene. In addition, based on the simulation studies, with a large π system and

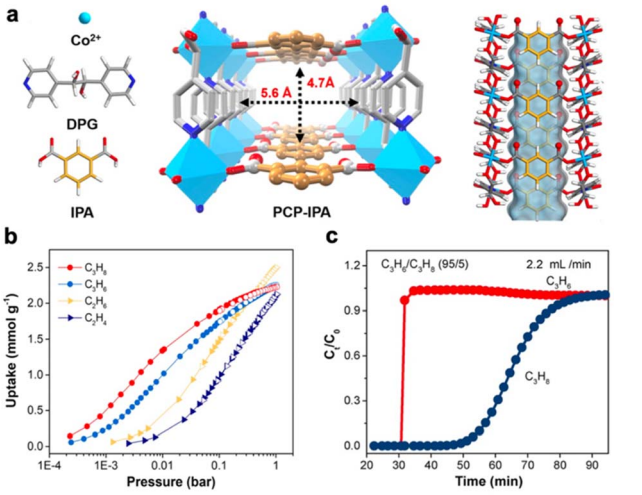

Fig. 8 Representative MOF (PCP-IPA) for propane-selective purification. (a) Schematic illustration of the building blocks and the 3D network topology of PCP-IPA, and the 1D channel structure of PCP-IPA. (b) Single-component adsorption–desorption isotherms of propane/propylene adsorption isotherms at 298 K. (c) Dynamic breakthrough curves of a propane/propylene mixture at 298 K and 1 bar. Reproduced with permission.[35] Copyright 2022, Springer Nature.

hydrogen bond acceptor provided by the aromatic units and uncoordinated negatively charged oxygen atoms, the straight channel of PCP-IPA acts as an efficient propane nano-trap.

5. Summary and outlook

In this highlight, we have summarized the latest advancements in propane/propylene separation by metal–organic frameworks. The major research progress based on two opposite preferences of gas adsorption: propylene-selective and propane-selective adsorption for propylene purification is presented. The separation performance and mechanism of representative examples of MOFs in each category are discussed and structure–property relationships are emphasized. Efficient separation of propylene and propane is of paramount importance in the petrochemical industry to produce high-purity propylene. In recent years, MOFs have stood out as excellent candidates for adsorptive separation of propane and propylene, which hold promise to replace or supplement the traditional heat-driven processes.

The potential of MOFs for propane/propylene separation has been well illustrated in this highlight article. However, some concerns and challenges need to be addressed in the future development of MOFs for their implementation in industrial separations. First, the trade-off between adsorption capacity and selectivity must be considered. As summarized in the article, most reported MOFs exhibit either exceptionally high adsorption uptake or adsorption selectivity for propane/propylene separation, but rarely possess high values for both. More powerful strategies based on reticular chemistry need to be established to guide the design of MOFs with optimal pore structure and chemistry and thus overcome this obstacle properly. Second, the stability and long-term recyclability of MOFs are extremely important aspects to be considered besides superior separation performance, particularly for practical applications at the industrial scale. Although tremendous advances in the design of MOFs with excellent separation performance have been achieved over the past three decades, most MOFs still suffer from poor thermal/chemical stability which further restricts their implementation in industries. The complicated separation conditions under the real-world settings (*e.g.*, high moisture, corrosively acidic environment, and relatively high temperature) require adsorbents with exceptionally high thermal and chemical stability as well as long-term recyclability. In this context, various approaches, including introducing early transition metals as inorganic building units and creating relatively high coordination numbers and connectivity in the structures, should be continuously explored. Most MOFs reported to date with competitive performance are built on expensive organic ligands, synthesized in organic solvents and often under complicated conditions, which vastly restrict their industrial implementation. In addition, reactions of MOFs are typically carried out at milligram scale in the laboratory settings, which would be unsuitable for real-world applications. Our recent work on the scale-up synthesis of Y-abtc and breakthrough experiments for the propylene/propane separation at large-scale serve as a good example for preparing materials for use at the industrial scale.[52] Thus, future efforts toward low-cost and large-scale production and green synthesis of MOFs are very important in facilitating the implementation of MOFs in industrial separation processes.

It is exciting to witness the remarkable progress over the recent years in the development of MOFs for highly efficient separation of propane and propylene. Particularly, several MOFs that are capable of selective adsorption of propane over propylene have been achieved for one-step propylene purification. However, the pursuit of propane-selective adsorption based on the cost-effective and highly stable MOFs remains an urgent and challenging task. Advanced strategies to achieve optimal pore confinement in MOFs to directly trap targeted propane molecules are of great significance. One of the strategies that may effectively enhance the adsorption selectivity of propane is systematic modulation of the pore chemistry and/or pore geometry.

Overall, despite the existing difficulties and challenges, we believe that with the rapid progress in MOF related research and development, many more candidates with further improved propane/propylene separation performance will be discovered. Moreover, newly developed state-of-the-art computational techniques such as machine learning have shown great potential to expedite the screening of MOF candidates and guide material synthesis. We have every reason to believe that MOFs will someday be implemented for the practical separation of propane and propylene.

Conflicts of interest

There are no conflicts to declare.

Acknowledgements

FX and JL would like to thank the U.S. Department of Energy, Office of Science, Office of Basic Energy Sciences (Grant No. DE-

SC0019902) for supporting this work. HW would like to acknowledge the financial support from Shenzhen Science and Technology Program (No. RCYX20200714114539243).

Notes and references

1 S. Chu, Y. Cui and N. Liu, *Nat. Mater.*, 2017, **16**, 16–22.
2 H. Jarvelin and J. R. Fair, *Ind. Eng. Chem. Res.*, 1993, **32**, 2201–2207.
3 D. S. Sholl and R. P. Lively, *Nature*, 2016, **532**, 435–437.
4 V. F. Martins, A. M. Ribeiro, M. G. Plaza, J. C. Santos, J. M. Loureiro, A. F. Ferreira and A. E. Rodrigues, *J. Chromatogr. A*, 2015, **1423**, 136–148.
5 S. U. Rege and R. T. Yang, *Chem. Eng. Sci.*, 2002, **57**, 1139–1149.
6 H. Wang, X. Dong, V. Colombo, Q. Wang, Y. Liu, W. Liu, X. L. Wang, X. Y. Huang, D. M. Proserpio and A. Sironi, *Adv. Mater.*, 2018, **30**, 1805088.
7 B. Liang, X. Zhang, Y. Xie, R.-B. Lin, R. Krishna, H. Cui, Z. Li, Y. Shi, H. Wu, W. Zhou and B. Chen, *J. Am. Chem. Soc.*, 2020, **142**, 17795–17801.
8 E. Worrell, D. Phylipsen, D. Einstein and N. Martin, *Energy Use and Energy Intensity of the US Chemical Industry*, Lawrence Berkeley National Lab.(LBNL), Berkeley, CA (United States), 2000.
9 K. Li and M. Beaver, *Advanced Nanostructured Molecular Sieves for Energy Efficient Industrial Separations*, Rive Technology, Inc., 2012.
10 K. Blok, M. Patel and T. Ren, *Faculty of Chemistry*, Utrecht University, 2006.
11 Y. Chen, Y. Yang, Y. Wang, Q. Xiong, J. Yang, S. Xiang, L. Li, J. Li, Z. Zhang and B. Chen, *J. Am. Chem. Soc.*, 2022, **144**, 17033–17040.
12 H. Wang, Y. Liu and J. Li, *Adv. Mater.*, 2020, **32**, 2002603.
13 H. Wang and J. Li, *Acc. Chem. Res.*, 2019, **52**, 1968–1978.
14 W. Fan, X. Zhang, Z. Kang, X. Liu and D. Sun, *Coord. Chem. Rev.*, 2021, **443**, 213968.
15 D. Saha, B. Toof, R. Krishna, G. Orkoulas, P. Gismondi, R. Thorpe and M. L. Comroe, *Microporous Mesoporous Mater.*, 2020, **299**, 110099.
16 P. J. Bereciartua, Á. Cantín, A. Corma, J. L. Jordá, M. Palomino, F. Rey, S. Valencia, E. W. Corcoran Jr, P. Kortunov and P. I. Ravikovitch, *Science*, 2017, **358**, 1068–1071.
17 R.-B. Lin, S. Xiang, W. Zhou and B. Chen, *Chem*, 2020, **6**, 337–363.
18 F. Xie, H. Wang and J. Li, *Matter*, 2022, **5**, 2516–2518.
19 H. Wang, D. Luo, E. Velasco, L. Yu and J. Li, *J. Mater. Chem. A*, 2021, **9**, 20874–20896.
20 H. C. Zhou, J. R. Long and O. M. Yaghi, *Chem. Rev.*, 2012, **112**, 673–674.
21 H. Furukawa, K. E. Cordova, M. O'Keeffe and O. M. Yaghi, *Science*, 2013, **341**, 1230444.
22 W. G. Cui, T. L. Hu and X. H. Bu, *Adv. Mater.*, 2020, **32**, 1806445.
23 K. Adil, Y. Belmabkhout, R. S. Pillai, A. Cadiau, P. M. Bhatt, A. H. Assen, G. Maurin and M. Eddaoudi, *Chem. Soc. Rev.*, 2017, **46**, 3402–3430.
24 H. Wang, X. Dong, J. Lin, S. J. Teat, S. Jensen, J. Cure, E. V. Alexandrov, Q. Xia, K. Tan and Q. Wang, *Nat. Commun.*, 2018, **9**, 1–11.
25 N. Nijem, H. Wu, P. Canepa, A. Marti, K. J. Balkus Jr, T. Thonhauser, J. Li and Y. J. Chabal, *J. Am. Chem. Soc.*, 2012, **134**, 15201–15204.
26 H. Wang, X. Dong, E. Velasco, D. H. Olson, Y. Han and J. Li, *Energy Environ. Sci.*, 2018, **11**, 1226–1231.
27 J.-X. Wang, C.-C. Liang, X.-W. Gu, H. Wen, C. Jiang, B. Li, G. Qian and B. Chen, *J. Mater. Chem. A*, 2022, **10**, 17878–17916.
28 X. Wang, R. Krishna, L. Li, B. Wang, T. He, Y.-Z. Zhang, J.-R. Li and J. Li, *Chem. Eng. J.*, 2018, **346**, 489–496.
29 Z. Chang, R.-B. Lin, Y. Ye, C. Duan and B. Chen, *J. Mater. Chem. A*, 2019, **7**, 25567–25572.
30 Y. Wang, N. Y. Huang, X. W. Zhang, H. He, R. K. Huang, Z. M. Ye, Y. Li, D. D. Zhou, P. Q. Liao and X. M. Chen, *Angew. Chem.*, 2019, **131**, 7774–7778.
31 X. Wang, P. Zhang, Z. Zhang, L. Yang, Q. Ding, X. Cui, J. Wang and H. Xing, *Ind. Eng. Chem. Res.*, 2020, **59**, 3531–3537.
32 L. Yu, X. Han, H. Wang, S. Ullah, Q. Xia, W. Li, J. Li, I. Da Silva, P. Manuel and S. Rudić, *J. Am. Chem. Soc.*, 2021, **143**, 19300–19305.
33 H. Zeng, M. Xie, T. Wang, R.-J. Wei, X.-J. Xie, Y. Zhao, W. Lu and D. Li, *Nature*, 2021, **595**, 542–548.
34 X. Li, J. Liu, K. Zhou, S. Ullah, H. Wang, J. Zou, T. Thonhauser and J. Li, *J. Am. Chem. Soc.*, 2022, **144**, 21702–21709.
35 P. Zhang, L. Yang, X. Liu, J. Wang, X. Suo, L. Chen, X. Cui and H. Xing, *Nat. Commun.*, 2022, **13**, 1–8.
36 E. D. Bloch, W. L. Queen, R. Krishna, J. M. Zadrozny, C. M. Brown and J. R. Long, *science*, 2012, **335**, 1606–1610.
37 J. E. Bachman, M. T. Kapelewski, D. A. Reed, M. I. Gonzalez and J. R. Long, *J. Am. Chem. Soc.*, 2017, **139**, 15363–15370.
38 T. M. Nicholson and S. K. Bhatia, *J. Phys. Chem. B*, 2006, **110**, 24834–24836.
39 N. Lamia, M. Jorge, M. A. Granato, F. A. A. Paz, H. Chevreau and A. E. Rodrigues, *Chem. Eng. Sci.*, 2009, **64**, 3246–3259.
40 J.-W. Yoon, I.-T. Jang, K.-Y. Lee, Y.-K. Hwang and J.-S. Chang, *Bull. Korean Chem. Soc.*, 2010, **31**, 220–223.
41 Y. Xie, Y. Shi, H. Cui, R.-B. Lin and B. Chen, *Small Struct.*, 2022, **3**, 2100125.
42 J. Li, X. Han, X. Kang, Y. Chen, S. Xu, G. L. Smith, E. Tillotson, Y. Cheng, L. J. McCormick McPherson and S. J. Teat, *Angew. Chem., Int. Ed.*, 2021, **60**, 15541–15547.
43 X.-W. Zhang, D.-D. Zhou and J.-P. Zhang, *Chem*, 2021, **7**, 1006–1019.
44 S. Tu, L. Yu, Y. Wu, Y. Chen, H. Wu, L. Wang, B. Liu, X. Zhou, J. Xiao and Q. Xia, *AIChE J.*, 2022, **68**, e17551.
45 Y. Chen, S. Tu, P. Fu, H. Wu, X. Wang, Y. Wu, Z. Li and Q. Xia, *AIChE J.*, 2022, e17730.
46 Q. Ding, Z. Zhang, P. Zhang, X. Cui, C.-H. He, S. Deng and H. Xing, *Chem. Eng. J.*, 2022, **434**, 134784.

47 Y. Chen, H. Wu, L. Yu, S. Tu, Y. Wu, Z. Li and Q. Xia, *Chem. Eng. J.*, 2022, **431**, 133284.
48 A. N. Hong, H. Yang, T. Li, Y. Wang, Y. Wang, X. Jia, A. Zhou, E. Kusumoputro, J. Li and X. Bu, *ACS Appl. Mater. Interfaces*, 2021, **13**, 52160–52166.
49 M. Chang, J. Ren, Y. Wei, J.-X. Wang, Q. Yang, D. Liu and J.-F. Chen, *Sep. Purif. Technol.*, 2021, **279**, 119656.
50 S.-Q. Yang, F.-Z. Sun, R. Krishna, Q. Zhang, L. Zhou, Y.-H. Zhang and T.-L. Hu, *ACS Appl. Mater. Interfaces*, 2021, **13**, 35990–35996.
51 S. J. Geier, J. A. Mason, E. D. Bloch, W. L. Queen, M. R. Hudson, C. M. Brown and J. R. Long, *Chem. Sci.*, 2013, **4**, 2054–2061.
52 E. Velasco, S. Xian, L. Yu, H. Wang and J. Li, *Sep. Purif. Technol.*, 2022, **282**, 120010.